Optimized Threshold-Voltage MOS Transistor Compact Model from the 4-Component Theory

Bin B Jie and Chih-Tang Sah

Florida Solid-State Electronics Laboratory
P O Box 116200, 335 Benton Hall, University of Florida
Gainesville, Florida 32611-6200, binjie@ufl.edu

ABSTRACT

A new optimized threshold-voltage compact model is derived from the 1996-Sah four-component-current theory for long channel MOS field-effect transistors. The self-consistent remote charge-neutrality boundary condition in the x-direction is used for the first time. Four independent optimization voltage parameters are proposed, one for each of the four current components (the parabolic space-charge-limited drift current, the bulk-charge depressment of the drift current, the linear space-charge-limited diffusion current, and the bulk-charge enhancement of the diffusion current**)**. The parameter values are obtained by least-squares-fit of each of the four current components from the compact model to that of the non-compact 4-component theory, from zero to the drain saturation voltage. The deviation is less than 4% in the strong inversion range.

Keywords: MOSFET, MOST, MOS transistor, compact model, space-charge-limited current, four-component theory, threshold voltage model.

1 INTRODUCTION

Design of MOS integrated circuits containing many transistors requires compact (simple and fast but still accurate) transistor models for use in the circuit simulator. The industrial standard MOS transistor compact models for the past decades have been the **threshold-voltage model** and its improvements to include diffusion current, mobility variations, hot carrier effects, and small geometry effects [1, 2]. Advanced compact models have been under recent development to meet new technologies and applications such as analog circuits and down-scaled and new transistor structures. These advanced models follow two approaches [3]: the **inversion charge** compact models (or the traditionally known **charge control modeling**) and the general **surface potential** compact models. This paper reports the initial test results of a new and optimized threshold-voltage compact model which is derived from the recently proposed four-component drain-current theory 1996-Sah [4,5,6] using the industrial standard bench-mark, the double-integral 1966-Pao-Sah [7], as the reference.

2 THE FOUR-COMPONENT MODEL

2.1 The 4-Component Formula

The 1996-Sah 4-component drain current formula for long-channel MOS transistors was given by [4**,** 5**,** 6]:

$$\begin{aligned}\frac{I_D L}{\mu_n Z} = \frac{C_O}{2}\left\{[V_{GX}-V_{FB}-V(0,0)]^2-[V_{GX}-V_{FB}-V(0,L)]^2\right\}\\ -\int_0^L\int_0^\infty q\,(P_B-P)(-E_Y)\,dxdy\\ +\tfrac{kT}{q}[V(0,L)-V(0,0)]C_O\\ +\tfrac{kT}{q}[Q_P(0,L)-Q_P(0,0)]\\ +\tfrac{1}{2}\varepsilon_S\int_0^L\int_0^\infty\frac{\partial}{\partial y}\left(E_Y^2-E_X^2\right)dxdy\\ +\tfrac{kT}{q}\varepsilon_S\int_0^\infty\left(\left.\frac{\partial E_Y}{\partial y}\right|_{y=L}-\left.\frac{\partial E_Y}{\partial y}\right|_{y=0}\right)dx\end{aligned} \quad (1)$$

Here $Q_P(0,y)=\int q(P_B-P)dx$ is the bulk charge. $V(0,y)$ is the surface potential at the source $V(0,y=0)=V_{S0}$ or at the drain $V(0,y=L)=V_{SL}$. The two terms of the first line in (1) are the parabolic space-charge-limited drift current; the second line, the bulk-charge depressment of the drift current; the third line, the linear space-charge-limited diffusion current; the fourth line, the bulk-charge enhancement of the diffusion current; the last two lines are short-channel and 2-D effects, and are neglected in this long-channel analysis.

2.2 Exact Iteration Algorithm for Surface Potential Computation

In order to evaluate the 4 components in (1), surface potential must be computed at each given gate voltage V_{GB}. In order to contrast the 4 components computed from the proposed compact model, we shall call the non-compact 4 components from [4, 5, 6] as the "exact" 4 components for the rest of this paper within the context of 1-D model. The dependence of the surface potential on the applied gate voltage is obtained from two implicit equations, both from integrating the Poison equation, one along the x-axis to give the Gauss Law, and the second, also along the x-axis but by quadrature to give the x-component of the electric field that appears in the Gauss Law. Assumptions are made to enable the two x-directed integrations including no recombination, no hole current, and electron current confined in the y-direction in order to give the x-independent electron and hole electrochemical or quasi-Fermi potentials (normalized to kT/q) $U_P(x,y) = U_P(y)$ and $U_N(x,y) = U_N(y)$ [8]. The remote boundary conditions at $x = \infty$ are: zero potential reference, zero x-component electric field, and the **self-consistent** or "exact" **charge neutrality condition** [9],

which is used for the first time in MOST analysis here and also by Zhou, et. al. [10]. This correct remote charge neutrality boundary condition was first arrived at empirically by McAndrew [11] without considering explicitly charge-neutrality. The minority carriers must be included to give the physical-real result at flatband that avoids the imaginary electric field as observed by recent authors [11,12,13] who used the not-self-consistent 1965-Sah-Pao [8] **(**also used 1966-Pao-Sah [7]) formula. The self-consistent x-independent electron and hole quasi-Fermi potentials are given by:

$$\exp(+U_P) = \sqrt{\left(\frac{P_{IM}}{2n_i}\right)^2 + \exp(U_{PN})} + \frac{P_{IM}}{2n_i}$$
$$\exp(-U_N) = \sqrt{\left(\frac{P_{IM}}{2n_i}\right)^2 + \exp(U_{PN})} - \frac{P_{IM}}{2n_i} \qquad (2)$$

Here $P_{IM} = P_{AA} - N_{DD}$ is the space-constant net p-type impurity concentration, $U_{PN} = U_{PN}(x,y) = U_{PN}(y)$ = voltage applied to the p+Drain $U_{PN}(y=L)=U_{DB}$ or to the p+Source $U_{PN}(y=0)=U_{SB}$ relative to n-Base of pMOST. (Negative sign for nMOST: $U_{PN}(y=L)=-U_{DB}$ and $U_{PN}(y=0)=-U_{SB}$)

The exact fast convergent iteration formulas for p-Base to obtain the surface potential U_S at a given U_{GX} or U_{GB} are:

$$F_S^2 = \frac{kT\,C_{OX}^2}{2q^2 n_i \varepsilon_S}(U_{GX} - U_{FB} - U_S)^2 \qquad (3)$$

Accumulation range ($U_S < -0.1$)

$$\Delta_A = 1 + \frac{\exp(-U_N)[1-\exp U_S] - U_S \cdot P_{IM}/n_i}{\exp(+U_P)} \qquad (4a)$$

$$U_S = -\log_e[F_S^2/\exp(+U_P) + \Delta_A] \qquad (4b)$$

Flatband range ($-0.1 \le U_S \le +1$)

$$\Delta_0 = \frac{\exp(-U_N)[1-\exp U_S] + \exp(+U_P)[1-\exp(-U_S)]}{P_{IM}/n_i} \qquad (5a)$$

$$U_S = F_S^2/(P_{IM}/n_i) + \Delta_0 \qquad (5b)$$

Depletion range ($+1 < U_S \le U_P + U_N$)

$$\Delta_D = \frac{\exp(-U_N)[1-\exp U_S] + \exp(+U_P)[1-\exp(-U_S)]}{P_{IM}/n_i} \qquad (6a)$$

$$U_{IM} = \frac{q^2 P_{IM}\varepsilon_S}{2kTC_{OX}^2} \qquad (6b)$$

$$U_S = U_{GX} - U_{FB} + 2U_{IM}\left(1 - \sqrt{1 + (U_{GX} - U_{FB} - \Delta_D)/U_{IM}}\right) \qquad (6c)$$

Inversion range ($U_P + U_N < U_S$)

$$\Delta_I = 1 - \exp(-U_S)\left\{1 + \frac{\exp(+U_P)[1-\exp(-U_S)] - U_S \cdot P_{IM}/n_i}{\exp(-U_N)}\right\} \qquad (7a)$$

$$U_S = U_N + \log_e(F_S^2/\Delta_I) \qquad (7b)$$

3 OPTIMIZED COMPACT MODEL

3.1 Bulk Charge Approximation

We note that the two bulk charge terms in the four exact components in (1) are double (dxdy) and single (dx) integrals which must be computed numerically. For compact modeling, these two integrals must be reduced to analytical forms. For the 1965-Sah-Pao analyses [8] Sah derived an analytical approximation to the bulk charge integral $Q_P(0,y) = \int q(P_B\text{-}P)dx$ by breaking up the surface space-charge region into three layers. In addition, Sah [8] obtained the three bulk charge terms as function of quasi-Fermi potential difference U_{PN} rather than surface potential $V(0, y) = V_S(y)$, a point missed by most later authors.

$$Q_P(0,y) = \sqrt{2qP_{IM}\varepsilon_S}\left\{\left[2V_F - 3\tfrac{kT}{q} - V_{PN}(0,y)\right]^{+1/2} + 2\tfrac{kT}{q}\left[2V_F - \tfrac{kT}{q} - V_{PN}(0,y)\right]^{-1/2} - e^{-1}\tfrac{kT}{q}\left[2V_F + \tfrac{kT}{q} - V_{PN}(0,y)\right]^{-1/2}\right\} \qquad (8)$$

The major contribution comes from the first term in (8), which is from the uncompensated and ionized impurities in the depletion layer at the SiO_2/Si interface.

Equation (8) suggests that an effective surface potential Ψ can be defined as follows to enable analytical evaluation of the single and double integrals:

$$\Psi(0,y) = 2V_F + V_\theta(y) - V_{PN}(0,y) \qquad (9a)$$
$$Q_P(0,y) = \sqrt{2qP_{IM}\varepsilon_S\Psi(0,y)} \qquad (9b)$$

where $V_\theta(y)$ is the optimization potential. This is just the linear approximation in the inversion charge model first employed in 1965-Sah-Pao [8] and described by Brews in his exposition of the 1978-Brews charge sheet model [14].

3.2 Surface Potential Bulk Charge Model

Although effective surface potential $\Psi(0,y)$ has no explicit relationship with the surface potential V_S or $V(0,y)$, we will approximate $\Psi(0,y)$ by V_S. Then, (9b) gives:

$$Q_P(0,y) = \sqrt{2qP_{IM}\varepsilon_S V(0,y)} \qquad (10a)$$

$$\begin{aligned}&\int_0^L\int_0^\infty q[P_B - P](-E_Y)dxdy \\ &= \int_0^L\left(\int_0^\infty q[P_B - P]dx\right)\frac{\partial V(0,y)}{\partial y}dy \\ &= \int_{V(0,0)}^{V(0,L)}\sqrt{2qP_{IM}\varepsilon_S V(0,y)}\,dV(0,y) \\ &= \sqrt{2qP_{IM}\varepsilon_S}\,\frac{2}{3}\left[V(0,L)^{3/2} - V(0,0)^{3/2}\right]\end{aligned} \qquad (10b)$$

Using (10a) and (10b), then (1) gives [6]

$$\begin{aligned}\frac{I_D L}{\mu_n Z} = \frac{C_O}{2}&\left\{[V_{GX} - V_{FB} - V(0,0)]^2 - [V_{GX} - V_{FB} - V(0,L)]^2\right\} \\ &- \sqrt{2qP_{IM}\varepsilon_S}\,\tfrac{2}{3}\left[V(0,L)^{3/2} - V(0,0)^{3/2}\right] \\ &+ C_O\tfrac{kT}{q}[V(0,L) - V(0,0)] \\ &+ \sqrt{2qP_{IM}\varepsilon_S}\,\tfrac{kT}{q}\left[V(0,L)^{1/2} - V(0,0)^{1/2}\right]\end{aligned} \qquad (11)$$

3.3 Optimized Compact Model

Using $\Psi(0,y)=V(0,y)$, (9a) and (11), (11) then give the compact model equation, (12), for the drain current with four optimization parameters, P_1, P_2, D_1 and D_2. Their numerical values are determined by least squares fit to the corresponding terms in the non-compact 1996-Sah formula given in (1). It is obvious that this is a threshold-voltage model with a peak in I_D therefore it must be cut off at the drain current saturation point or at the peak, a deficiency,

but it includes the diffusion current terms which dominate in the subthreshold or weak inversion range of gate biases.

$$\begin{aligned}\frac{I_D L}{\mu_n Z} = \frac{C_O}{2}\Big\{&[V_{GX} - V_{FB} - V_{SX} - 2V_F - P_1]^2 \\ &- [V_{GX} - V_{FB} - V_{DX} - 2V_F - P_1]^2\Big\} \\ &- \sqrt{2qP_{IM}\varepsilon_S}\,\tfrac{2}{3}\Big[[V_{DX} + 2V_F + P_2]^{3/2} - [V_{SX} + 2V_F + P_2]^{3/2}\Big] \\ &+ C_O\,\tfrac{kT}{q}[V_{DS} + D_1] \\ &+ \sqrt{2qP_{IM}\varepsilon_S}\,\tfrac{kT}{q}\Big[[V_{DX} + 2V_F + D_2]^{1/2} - [V_{SX} + 2V_F + D_2]^{1/2}\Big]\end{aligned} \quad (12)$$

3.4 Extraction of 4 Optimization Parameters

The four optimization parameters can be individually optimized over the device-operation domain (V_G, V_D, V_S, $V_X \equiv V_B$) and the device-design domain (P_{IM}, X_{OX}), by least squares fit of each of the four compact-model components of (12) to the corresponding exact component of (1).

After obtaining the values of the four optimization parameters over both operation and design domains by a one-time effort to create a two-dimensional table, the optimized compact model can then be used to fit experimental characteristics by variation of the two effective device design parameters (P_{IM}, X_{OX}). Since X_{OX} is usually determined accurately by C-V or other experimental methods, we are left with only one parameter to fit the experiment, which is P_{IM}, the effective net impurity concentration in the basewell. It is an electrical average over both x and y directions for ion implants.

4 I-V CHARACTERISTICS

Using the exact remote charge neutrality boundary condition (2), surface potentials are computed for a given gate voltage V_{GB} and a range of $V_{PN}(y)$ from the source $V_{PN}(y=0) = -V_{SB}$ to the drain $V_{PN}(y=L) = -V_{DB}$ for the y-integration using the fast convergent but still exact formulas (3) to (7b) over the accumulation, flatband, depletion and inversion ranges without negative number inside the square root near flatband observed by [10-13].

Then, the 1966-Pao-Sah double integral [7] and the exact 4-component formula (1) are computed and the %-deviation labeled CTS96XT is shown in Fig. 1 which also shows (CTS9604BJ [6]) the deviation of the drain current computed from the surface potential bulk charge non-compact model formula (11). These curves in Fig. 1 show that the 1996-Sah exact 4-component formula is about 1% smaller than the 1966-Pao-Sah double integral formula. The reasons have yet been delineated by us. The curves in Fig. 1 also show this bulk charge model is about 3%-5% smaller than the 1966-Pao-Sah which is better than a number of other compact models.

Figure 2 shows the drain current components and total drain current of both exact 4-component formula (labeled XT) and optimized compact model (labeled CM) at one device-design domain point ($5x10^{17}cm^{-3}$, 5.0nm) with the gate voltage $V_{GX} - V_{FB} = 5.0V$. Figure 3 shows the corresponding percentage deviation of Fig. 2. In most part of linear region V_{DS} = (0 V, 2.6 V), the deviations of four components are less than 4%.

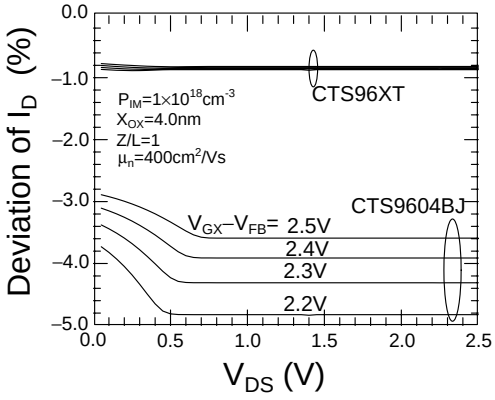

Figure1: Percentage drain current deviation of exact 4-componet formula (labeled CTS96XT) and surface potential bulk charge model (labeled CTS9604BJ) compared with Pao-Sah double integral.

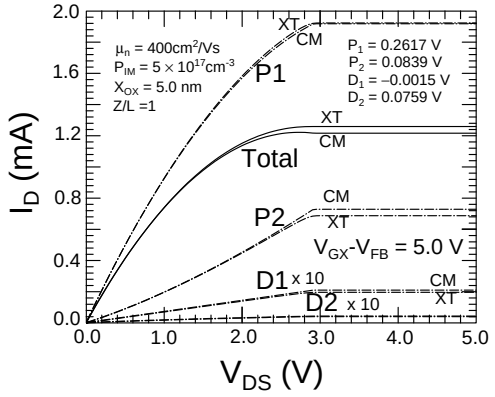

Figure 2: Output characteristics of 4 components (P1, P2, D1, D2) and total drain current from the exact 4-compact formula (XT) and the optimized compact model (CM).

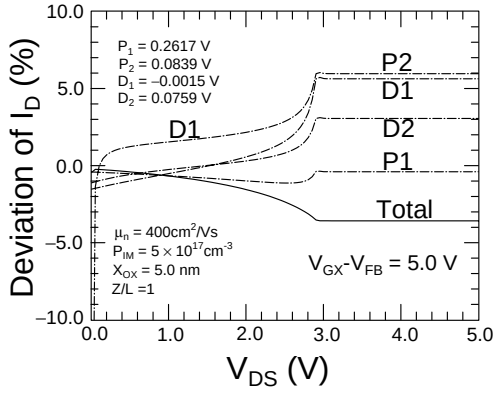

Figure 3: Drain current percentage deviation of the optimized compact model compared with the exact 4-component formula versus the drain voltage.

Figure 4 shows the four optimization parameters P_1, P_2, D_1, and D_2, versus the gate voltage at the device-design domain point ($5x10^{17}$ cm^{-3}, 5.0nm). It shows that optimization parameters P_1 and D_1 of the space-charge-limited parabolic drift and linear diffusion components have weak dependences on gate voltage, while the two bulk-charge-limited optimization parameters, P_2 and D_2, have strong dependences on gate voltage. These are understood by comparing the two current equations, (11) and (12):

(1) The gate voltage dependence of the four optimization parameters in (12) are expected since these parameters originated from the optimization potential V_θ in (9a) with an assumed linear interdependence of the surface potential and the quasi-Fermi potential difference.

(2) On the space-charge-limited drift component, gate voltage dependence of surface potential in the strong inversion range is less than $f(V_{GX}) = V_{GX}$, thus the optimization parameter P_1 is a weak function of V_{GX}.

(3) On the space-charge-limited diffusion component, gate voltage dependences of the surface potentials at source and at drain cancel each other, thus optimization parameter D_1 is a weak function of gate voltage.

(4) Both bulk-charge-limited components, P_2 and D_2 are functions of gate voltage. But in the optimized compact model they have no explicit gate voltage dependence**,** hence their gate voltage dependences are through the optimization parameters.

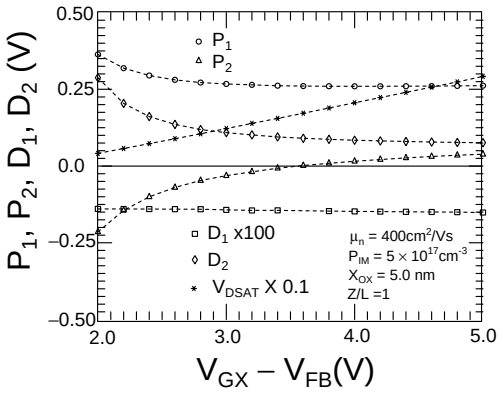

Figure 4: The four optimization parameters extracted over drain voltage range (0, V_{DSAT}) versus gate voltage.

5 CONCLUSION

From the 1996-Sah exact 4-component formula, two types of compact models are derived. One was the **surface potential** bulk-charge model, CTS9604BJ [6]. The second, treated in this paper, is a **threshold-voltage** bulk-charge model, or the **optimized** compact model, CTS9604BJ-CM. An exact iteration algorithm for computing the surface potential at a given gate voltage is described, using the exact remote charge-neutrality boundary condition for the first time. Compared with 1966-Pao-Sah double integral, the 1996-Sah 4-component formula shows about 1% deviation with unidentified reasons.

For this optimized threshold-voltage compact model, CTS9604BJ-CM, the deviations are within 4% of those of the exact 1996-Sah 4-component formula CTS96XT. The gate voltage dependences of four optimization parameters are discussed which are critical for modeling subthreshold range of the drain current, which will be reported.

REFERENCES

[1] Narain Arora, *MOSFET Models for VLSI Circuit Simulation*, *Theory and Practice*, Springer-Verlag, Wien, New York, 1993, Chapter 6, pp230-324. (**1993-Arora**)

[2] Chih-Tang Sah, "A history of MOS Transistor Compact Modeling," Proceedings, this conference.

[3] Josef Watts, Colin McAndrew, and 8 co-authors, "Advanced compact models for MOSFETs," Proceedings, this conference. (**2005-Watts-McAndrew+8**)

[4] Chih-Tang Sah, "Space-Charge Theory of the MOS Transistor," December 12, 1996 and March 31, 1997. Publication planned. To be referred to as 1996-Sah and **CTS96XT** where XT stands for "exact".

[5] Bin B. Jie and Chih-Tang Sah, "Physics-based exact analytical drain current equation and optimized compact model for long channel MOS transistors," Proceedings of 7th ICSICT, 911-945, October 18-21, 2004, Beijing. IEEE Catalog No. 04EX863. (**CTS9604BJ**)

[6] Bin B Jie and Chih-Tang Sah, "Evaluation of a surface-potential-based bulk-charge model for MOS transistors," submitted to IEEE TED. (**CTS9604BJ**)

[7] H. C. Pao and C-T Sah, "Effects of diffusion current on the characteristics of metal-oxide-semiconductor transistors," Solid-State Electronics, 9(10), 927-937, October 1966. (**1966-Pao-Sah**)

[8] Chih-Tang Sah and Henry C. Pao, "The effects of fixed bulk charge on the characteristics of metal-oxide-semiconductor transistors," IEEE Trans. ED-13(4), 393-405, April 1966. (**1965-Sah-Pao**)

[9] Chih-Tang Sah, Robert N. Noyce, and William Shockley, "Carrier generation and recombination in p-n junctions and p-n junction characteristics," Proc. IRE, vol. 55(9), 1228-1345, 1957. Eq. (58) in appendix. (**1957-SNS**)

[10] Xing Zhou, et. al., "Unified regional charge-based versus surface-potential-based compact modeling approaches," Proceedings of this Conference.

[11] Colin C. McAndrew and James J. Victory, "Accuracy of approximations in MOSFET charge models," IEEE Trans. ED-49(1), p. 72, January 2002.

[12] Weimen Wu, T-L Chen, G. Gildenblat, C. C. McAndrew, "Physics-based mathematical conditioning of the MOSFET surface potential equation," IEEE Trans. ED-51(7), 1196-1200, December 2004

[13] Rafael Rios, S. Mudanai, W-K Shih, Paul Packan, "An efficient surface potential solution algorithm for compact MOSFET models," IEDM Tech. Dig. 755-758, 2004.

[14] J. R. Brews, "A charge-sheet model of the MOSFET," Solid-State Electronics 21(2), pp.345-355, October 1978. (**1978-Brews**)